

Molecular Relaxation Spectroscopy of Flavin Adenine Dinucleotide in Wild Type and Mutant Lipoamide Dehydrogenase from *Azotobacter vinelandii*[†]

Philippe I. H. Bastiaens,[†] Arie van Hoek,[§] Willem J. H. van Berkel,[‡] Aart de Kok,[‡] and Antonie J. W. G. Visser^{*‡}

Departments of Biochemistry and Molecular Physics, Agricultural University, P.O.Box 8128, 6700 ET Wageningen, The Netherlands

Received February 24, 1992; Revised Manuscript Received May 4, 1992

ABSTRACT: The temperature dependence of the fluorescence emission spectra of flavin adenine dinucleotide bound to lipoamide dehydrogenase from *Azotobacter vinelandii* shows that the protein matrix in the vicinity of the prosthetic group is rigid on a nanosecond time scale in a medium of high viscosity (80% glycerol). The active site of a deletion mutant of this enzyme, which lacks 14 C-terminal amino acids, is converted from a solid-state environment (on the nanosecond time scale of fluorescence) into a state where efficient dipolar relaxation takes place at temperatures between 203 and 303 K. In aqueous solution, fast dipolar fluctuations are observed in both proteins. It is shown from fluorescence quenching of the flavin by iodide ions that the prosthetic groups of the mutant protein are partially iodide accessible in contrast to the wild type enzyme. A detailed analysis of the temperature dependence of spectral energies according to continuous relaxation models reveals two distinct relaxation processes in the deletion mutant, which were assigned to solvent and protein dipoles, respectively. From the long-wavelength shifts of the emission spectra upon red-edge excitation, it is demonstrated that the active site of the wild type enzyme has high structural homogeneity in comparison to the deletion mutant. In combination with results obtained by X-ray diffraction studies on crystals of the wild type enzyme, it can be concluded that the C-terminal polypeptide of the *A. vinelandii* enzyme interacts with the dehydrolipoamide binding site, thereby shielding the flavins from the solvent.

Steady-state fluorescence spectroscopy has been extensively used to obtain information on structural and dynamical properties of biological macromolecules, since the spectral parameters of fluorescence emission such as position, shape, and intensity are dependent on the electronic and dynamic properties of the chromophore environment (Teale, 1960; Weber, 1960; MacGregor & Weber, 1981, 1986). During the last decade, a new approach has evolved to observe dipolar relaxation dynamics in the vicinity of fluorophores in proteins (Demchenko, 1982, 1985, 1986, 1987, 1988a). This technique exploits the possibility of photoselecting nonequilibrium solvates (solvate: fluorescent molecule and its immediate surrounding) by site-selective excitation at the red edge of the absorption band. The spectral parameters of the fluorescence emission are then dependent on the inhomogeneity of the electric field surrounding the fluorophores and on its relaxational properties as caused by temperature-dependent structural fluctuations of protein and solvent dipoles. This technique has been applied to obtain information on dipolar relaxation in the vicinity of the intrinsically fluorescent tryptophan residue in proteins (Demchenko, 1988b). It was found that proteins containing a tryptophan with either an extreme short- or long-wavelength-emission spectrum did not exhibit a long-wavelength shift upon red-edge excitation in contrast to proteins with an emission spectrum in the intermediate spectral region. The apolar nature of the chromophore environment in the short-wavelength emitting class of proteins results in a narrow distribution of interaction energies. The absence of a long-wavelength shift in this class of proteins indicated a negligible photoselection of nonequilibrium excited

states. In the long-wavelength emitting class, the absence of a spectral shift was explained because the chromophores were accessible to the rapidly fluctuating solvent dipoles, causing fluorescence emission to take place from the equilibrium excited state irrespective of excitation wavelength. In the mid-range emitting proteins, temperature- and excitation frequency-dependent shifts of the emission spectra were associated with dipolar relaxation with a characteristic time constant in the same order as the lifetime of the excited state. From the average dipolar relaxation time obtained from such experiments, the protein matrix surrounding a chromophore can be ranked from fluid to solid state on the time scale of fluorescence emission. These experiments, among others, demonstrate the potential of molecular relaxation spectroscopy to obtain information on dynamical properties near an extrinsic or intrinsic fluorophore in proteins.

No attempts have been made thus far to study dipolar relaxational properties in flavoproteins by investigating the fluorescence spectral emission characteristics of the intrinsically fluorescent prosthetic group FAD¹ or FMN. These fluorescent nucleotides exhibit different spectral characteristics in different flavoproteins, reflecting the specific environmental properties of the isoalloxazine, which is the relevant chromophore (Weber, 1950; Visser et al., 1974, 1984; Visser & Müller, 1979; Visser, 1989). In this study we present the structural and dynamic properties of the active sites in the flavoprotein lipoamide dehydrogenase from *Azotobacter vine-*

[†] This research was supported in part by The Netherlands Organization for Scientific Research (NWO).

* Author to whom correspondence should be addressed.

[‡] Department of Biochemistry.

[§] Department of Molecular Physics.

¹ Abbreviations: ADC, analog to digital converter; CW, continuous wavelength; EDTA, ethylenediaminetetraacetic acid; FAD, flavin adenine dinucleotide; LipDH, lipoamide dehydrogenase; LipDH-AV, lipoamide dehydrogenase from *Azotobacter vinelandii*; LipDH- Δ 14, deletion mutant of lipoamide dehydrogenase from *A. vinelandii*; Lip(SH₂), reduced lipoamide; MCA, multichannel analyzer; MCS, multichannel scaling; NAD⁺, nicotinamide adenine dinucleotide, oxidized form; SV, Stern-Volmer.

landii (LipDH-AV) as inferred from temperature-dependent laser-induced site-selective fluorescence emission spectroscopy. Lipoamide dehydrogenase belongs to the class of disulfide oxidoreductases and catalyses the NAD⁺-dependent oxidation of the covalently attached dihydrolipoyl groups of lipoate acyltransferase in different multienzyme complexes (Williams, 1976; Reed & Oliver, 1986; McCully et al., 1986). The dimeric 100-kDa protein possesses an $\alpha\alpha$ -quaternary structure where each subunit contains one highly fluorescent FAD cofactor (quantum yield 240% of that of free FAD). The gene encoding lipoamide dehydrogenase from *A. vinelandii* has been cloned and expressed in *Escherichia coli* TG2, which provides means to modify the active site near the isoalloxazine of FAD by site-directed mutagenesis (Westphal & de Kok, 1988). The last 10 C-terminal amino acids of the *A. vinelandii* enzyme are not visible in the electron density map of the high-resolution crystal structure, indicating that they are disordered (Schierbeek et al., 1989; Mattevi et al., 1991). From biochemical studies on a deletion mutant of the *A. vinelandii* enzyme, lacking the C-terminal 14 amino acids, it was concluded that the C-terminus has an important function in catalytic activity and stability of the dimer (Schulze et al., 1991). It is then possible that the C-terminal tail interacts with the lipoamide binding site, which comprises amino acid residues from both subunits, thereby stabilizing the dimer. In this respect we compared the solvent accessibility and the dipolar relaxational properties near the flavins of the deletion mutant (LipDH- Δ 14) and the wild type enzyme.

THEORY

Chromophores in an unstructured dipolar environment, such as a polar solvent, exhibit a statistical deviation of dipolar interaction energies around the equilibrium minimal interaction energy due to thermal motions of solvent molecules. This holds true for both ground and excited states of the chromophore, resulting in a distribution of singlet-singlet transition frequencies and inhomogeneous broadening of spectra (Rubinov & Tomin, 1970; Nemkovich et al., 1991). Excitation at the main band or red edge of the absorption spectrum results in the population of nonequilibrium Franck-Condon excited states. Site-selective excitation at the red edge of the absorption band photoselects chromophores with minimal electronic transition frequencies (Demchenko, 1986, 1987). The corresponding instantaneous emission spectrum will be shifted to long wavelengths relative to the spectrum obtained at main-band excitation (Rubinov & Tomin, 1970; Galley & Purkey, 1970). In both excitation regimes (red edge and main band), the excited solvates will have a tendency to relax to the minimal energy configuration with a characteristic dipolar relaxation time τ_r . According to the time-integrated continuous relaxation model of Bakshiev and Mazurenko, the relation between the mean wavenumber of the steady-state emission spectrum ($\bar{\nu}$), dipolar relaxation time (τ_r), and average fluorescence lifetime ($\bar{\tau}_f$) is (Mazurenko & Bakshiev, 1970)

$$\frac{\bar{\nu} - \bar{\nu}_\infty}{\nu_0 - \nu_\infty} = \frac{\Delta\nu}{\Delta\nu_0} = \frac{\tau_r}{\tau_r + \bar{\tau}_f} \quad (1)$$

When there is no motion of the dipoles of the chromophore environment on the time scale of fluorescence, τ_r is much longer than $\bar{\tau}_f$ and the unrelaxed spectrum is obtained with mean frequency $\bar{\nu}_0$. This spectrum is typically observed at low temperatures. In the reverse situation where τ_r is much longer than $\bar{\tau}_f$, practically all emission takes place from the equilibrium excited state and the relaxed spectrum with mean frequency $\bar{\nu}_\infty$ is obtained. This spectrum, typically observed

at elevated temperatures, is difficult to obtain for proteins due to temperature-induced denaturation and subsequent loss of tertiary structure. A useful expression which does not contain $\bar{\nu}_\infty$ was derived by assuming that τ_r , $\bar{\tau}_f$, and $\bar{\nu}_\infty$ are independent of excitation wavelength (Demchenko, 1982, 1985, 1986, 1987):

$$\frac{\bar{\nu} - \bar{\nu}^{\text{edge}}}{\bar{\nu}_0 - \bar{\nu}_0^{\text{edge}}} = \frac{\Delta\nu^{\text{edge}}}{\Delta\nu_0^{\text{edge}}} = \frac{\tau_r}{\tau_r + \bar{\tau}_f} \quad (2)$$

where $\bar{\nu}^{\text{edge}}$ is the mean wavenumber of the spectrum obtained upon red-edge excitation. From this expression, the dipolar relaxation time in biological molecules can be estimated from the ratio of the difference in mean frequency of the spectra upon main-band and red-edge excitation at a certain temperature. Maximal difference in mean frequency is obtained at low temperatures, where the dipolar relaxation is much slower than the fluorescence emission.

MATERIALS

LipDH-AV and the mutant LipDH- Δ 14 expressed in *E. coli* TG4 were purified as described before (Westphal & de Kok, 1988; Schulze et al., 1991). The enzyme preparations were frozen in liquid nitrogen and stored at -70°C in 100 mM K₂HPO₄, pH 7.0, 0.5 mM EDTA. The samples were defrosted at room temperature and 300- μL aliquots were chromatographed on a Biogel PGD-6 column (Bio-Rad, 1 \times 6 cm) equilibrated with 50 mM K₂HPO₄, pH 7.0, to eliminate unbound FAD. All buffers were made with nanopure water prepared on a Millipore water purification system. The enzyme preparations to be brought to 80% (v/v) glycerol were chromatographed as above except that the column was equilibrated with 250 mM K₂HPO₄, pH 7.0. From the eluted sample, 100 μL was gently mixed with 400 μL of 100% glycerol (Merck, fluorescent microscopy grade) until a homogeneous solution was obtained. Enzyme concentrations were determined with a molar extinction coefficient of $\epsilon_{457} = 11.3 \text{ mM}^{-1} \text{ cm}^{-1}$ (Westphal & de Kok, 1988). Care was taken that all final preparations had a concentration of 10–15 μM to ensure that the enzymes were in the dimeric form. FAD was purified on a Biogel P-2 (Bio-Rad). Aliquots (100 μL) of this preparation were mixed with 400 μL of glycerol to a final concentration of 10 μM . When the samples were frozen to 203 K, a clear transparent glass was formed with no indications of any precipitate.

INSTRUMENTATION

Emission spectra at different temperatures were obtained by excitation with light of 514.5- or 457.9-nm wavelength of a mode-locked cw argon ion laser (Coherent Radiation Model CR 18) emitting light pulses at a rate of 76 MHz. Samples were 0.5 cm³ in volume in 1-cm light path cuvettes, placed in a thermostated holder. This holder was placed in a sample housing also containing the optics.

A liquid nitrogen flow setup with a temperature controller (Oxford Model ITC4) was used for sample temperatures down to 203 K. At these low temperatures experiments can be easily disturbed by the condensation of water from the surrounding air on the cuvette. Therefore the sample housing was extended in height and filled with a steady stream of the relatively heavy argon gas onto the cuvette walls. The final temperature of the sample appeared to be in balance with different heat sources (cold nitrogen, room temperature argon gas, the heater of the controller, and heat radiation), and care

was taken to control the true sample temperature. Furthermore, the cuvettes were exchanged by wearing surgical gloves. In this way, experiments could be performed over a period of a few hours without dew and ice problems. A Glan laser polarizer was mounted at the front of the sample housing, optimizing the already vertical polarization of the input light beam. Between sample and photomultiplier (microchannel plate, Hamamatsu Model 1645U), a single fast lens (uncoated fused silica), a rotatable sheet polarizer, and a computer-controlled monochromator (two tandemized 0.25-m monochromators, $f/3.5$ Jarrel Ash Model 82.410) were placed. The sheet type polarizer in the detection pathway was placed under magic angle with respect to the polarization of the excitation light. Emission photons (via a constant-fraction discriminator, Canberra Model 1428A) were directly fed to the multichannel scaling (MCS) input of the multichannel analyzer (MCA, Nuclear Data Model ND66, equipped with both a ND582 ADC and a zero dead time multichannel scaling unit). The channel stepping of the MCS was time synchronized by the controller of monochromator's stepper motor. The bandwidth of the monochromator was 6 nm for the spectra with 457.9-nm excitation and 2 nm for the spectra with 514.5-nm excitation. Four spectra were acquired at every temperature and excitation wavelength in the range of 470–662 nm over 1024 channels. The emission spectra were converted from technical to molecular spectra in a computer program containing the transmission characteristics of the monochromator and the photomultiplier responses.

Fluorescence quenching experiments were performed on a SLM-Aminco SPF-500C fluorometer. The excitation wavelength was set at 450 nm and the emission at 550 nm. Both excitation and emission slits were set at 4-nm bandpass.

Time-resolved fluorescence measurements and analysis were performed as described elsewhere (Bastiaens et al. 1992).

COMPUTATIONAL METHODS

All emission spectra contained 1024 points and were linear on a wavelength scale (470–662 nm). The spectra were converted to a wavenumber scale by taking the reciprocal of the vector $\vec{\lambda}$, where each element λ_i is the discrete value of the corresponding wavelength in channel i of the MCA:

$$\vec{\nu} = 1/\vec{\lambda} \quad (3)$$

The center of gravity or mean wavenumber of a spectrum is then calculated by

$$\bar{\nu} = (\vec{\nu} \cdot \vec{I}) / |\vec{I}| \quad (4)$$

where each element I_i of the vector \vec{I} contains the number of counts in channel i of the MCA. Upon excitation at 514.5 nm (red-edge excitation), the spectra contained a peak of large amplitude spanning the channels 224–264 of the MCA (512–519 nm) which could be attributed to scattered light. In both the main-band and the red-edge excited emission spectra, these channels were omitted in the calculation of the center of gravity to obtain comparable results. Manipulation of the excitation and emission spectra (such as correction for instrumental distortions, calculation of the center of gravity of the fluorescence bands, and fitting to quenching and relaxation models) was performed on a Apple Macintosh SE/30 computer equipped with the program IGOR (Wavemetrics).

RESULTS

Fluorescence Quenching by Iodide. The solvent accessibility of the isoalloxazines in the wild type (LipDH-AV) and deletion

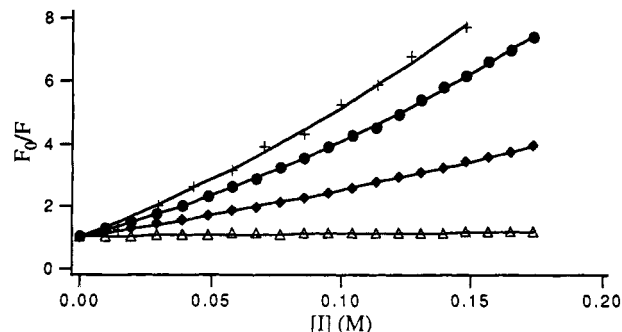


FIGURE 1: Stern-Volmer plots of iodide quenching of flavin fluorescence in LipDH-AV (Δ), LipDH- Δ 14 (\blacklozenge), free FAD (\bullet), and free FMN ($+$) in 50 mM KP_i , pH 7.0 at 293 K. The solid lines are the optimized fits of the data to the modified Stern-Volmer equation.

Table I: Fluorescence Quenching Parameters

	K_{sv} (M^{-1})	$\bar{\tau}_f$ (ns)	k_q ($M^{-1} ns^{-1}$)	V (M^{-1})
LipDH-AV	0.86 ± 0.06	2.0	0.43 ± 0.03	
LipDH- Δ 14	11.7 ± 0.2	1.1	9.9 ± 0.2	1.12 ± 0.04
FAD	20.9 ± 0.2	2.5^a	8.4 ± 0.1	2.74 ± 0.06
FMN	31.1 ± 2.0	4.7^a	6.6 ± 0.4	2.24 ± 0.41

^a Value obtained from Visser (1984).

mutant (LipDH- Δ 14) of lipoamide dehydrogenase were compared to that of the free chromophore by measuring the extent of collisional quenching of the flavin fluorescence by iodide ions. The data are represented in a Stern-Volmer plot (Figure 1) where the relative flavin fluorescence is plotted against the iodide concentration ($[I]$). The data were fitted to a modified Stern-Volmer equation to account for static quenching due to the presence of ions at the moment of excitation in the quenching sphere of action (V) (Eftink & Ghiron, 1981):

$$F_0/F = (1 + K_{SV}[I]) \exp([I]V) \quad (5)$$

where F_0 and F are the fluorescence intensities in the absence and presence of quencher, respectively. The Stern-Volmer quenching constant (K_{SV} in M^{-1}) is the product of the bimolecular quenching constant (k_q in $M^{-1} ns^{-1}$) and the lifetime of the chromophore ($\bar{\tau}_f$ in ns) in the absence of quencher. V is the effective volume around the chromophore (in dm^3) at which static quenching occurs per mole of fluorophore. The optimized parameters as obtained from the fit of the data are gathered in Table I, and the curves described by these parameters are represented in Figure 1 by the solid lines. Visual inspection of the Stern-Volmer plots as well as the larger bimolecular quenching constant indicates the increased iodide accessibility of the isoalloxazines in LipDH- Δ 14 in comparison with that in LipDH-AV. From the decreased effective volume of static quenching in LipDH- Δ 14 as compared to that of the free chromophore, one can conclude that flavin is partly shielded from iodide ions by the protein matrix. In the deletion mutant protein we thus expect an enhanced interaction of the flavin with solvent dipoles, and in this way the relaxational properties of the excited state of a chromophore inside a protein in distinct environments can be compared.

Spectral Shifts. We examined the emission spectra of free FAD and FAD bound to LipDH-AV and LipDH- Δ 14 in 80% glycerol and in aqueous solution as a function of temperature upon main-band (457.9 nm) and red-edge (514.5 nm) excitation. As can be seen in Figure 2A, the spectrum of FAD in 80% glycerol exhibits a considerable shift ($\Delta\nu = 600$ cm^{-1}) in the temperature region from 203 to 303 K at main-

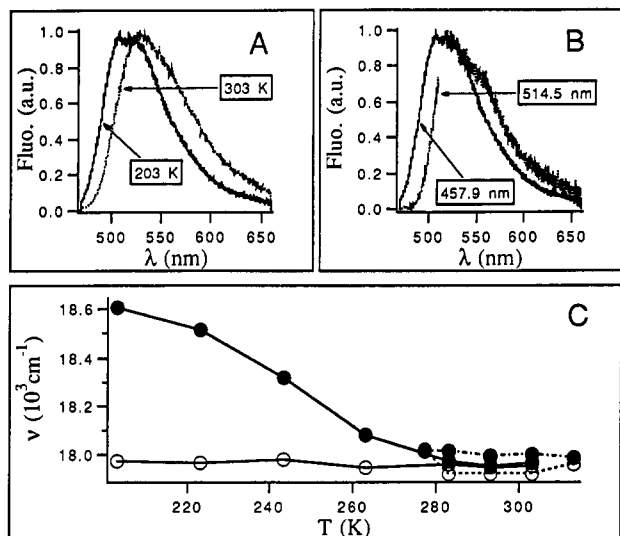


FIGURE 2: Temperature and excitation-wavelength dependence of fluorescence spectra of free FAD. (A) Temperature-dependent shift of emission spectra of free FAD in 80% glycerol, 50 mM KP_i , pH 7.0, upon 457.9-nm excitation. (B) Excitation-wavelength-dependent shift of emission spectra at 203 K in same solvent as in (A). The points between 512 and 519 nm contain a considerable amount of 514.5-nm laser scattering and were therefore omitted in the spectrum obtained after red-edge excitation. (C) Center of gravity expressed on a wavenumber scale as function of temperature and excitation wavelength: open symbols, 514.5-nm excitation; closed symbols, 457.9-nm excitation; solid lines, data obtained in 80% glycerol, 50 mM KP_i , pH 7.0; broken lines, data obtained in 50 mM KP_i , pH 7.0. Error bars are within the thickness of the experimental points.

band excitation. A similar long-wavelength shift of the spectrum is observed at 203 K at red-edge excitation (Figure 2B) which is completely abolished above 280 K. In aqueous solution, no substantial shifts were observed with temperature or upon red-edge excitation. The temperature dependence of the center of gravity of the emission spectra is represented in Figure 2C on a wavenumber scale. From Figure 2C it is clear that (i) site-selective excitation of nonequilibrium solvates takes place upon excitation at 514.5 nm at low temperature and (ii) the energy of the emitted photons is dependent on the dipolar relaxational properties of the solvent.

The spectral dependence of bound FAD in the wild type enzyme on temperature and excitation wavelength was completely different from that of the free chromophore. With an increase in temperature, the emission spectrum of LipDH-AV in 80% glycerol hardly shifts to longer wavelengths, upon main-band excitation (Figure 3A). A small bathochromic shift of the emission spectra could be detected upon red-edge excitation (Figure 3B). In Figure 3C, the center of gravity of the emission spectrum on a wavenumber scale has been plotted as a function of temperature. In aqueous solution the spectra were shifted to longer wavelengths relative to the spectra in 80% glycerol and did not show either a substantial temperature- or an edge excitation-induced shift (see symbols connected by broken lines in Figure 3C).

For LipDH- $\Delta 14$ we found a clear temperature and excitation-wavelength dependence of the emission spectra. Upon main-band excitation, a red shift of the emission spectra was apparent with increase of temperature (Figure 4A). Upon red-edge excitation at 203 K, the emission spectrum is shifted to longer wavelengths, relative to the spectrum obtained upon main-band excitation (Figure 4B). With an increase of temperature, the center of gravity of main-band and red-edge excited fluorescence spectra converge to the same wavenumber (Figure 4C), which shows that the active site of the protein

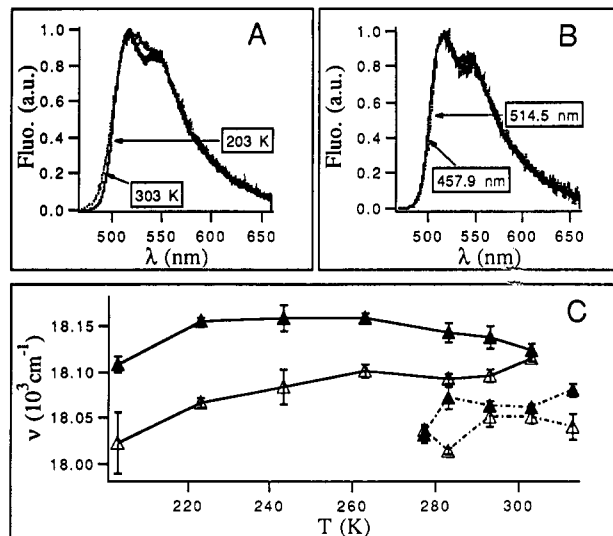


FIGURE 3: Temperature and excitation-wavelength dependence of emission spectra of wild type lipoamide dehydrogenase. (A) Temperature-dependent shift of emission spectra of FAD bound to LipDH-AV in 80% glycerol, 50 mM KP_i , pH 7.0, upon 457.9-nm excitation. (B) Excitation-wavelength-dependent shift of emission spectra at 203 K for same sample as in (A). The points between 512 and 519 nm contain a considerable amount of 514.5-nm laser scattering and were therefore omitted in the spectrum obtained after red-edge excitation. (C) Center of gravity expressed on a wavenumber scale as function of temperature and excitation wavelength: open symbols, 514.5-nm excitation; closed symbols, 457.9-nm excitation; solid lines, data obtained in 80% glycerol, 50 mM KP_i , pH 7.0; broken lines, data obtained in 50 mM KP_i , pH 7.0.

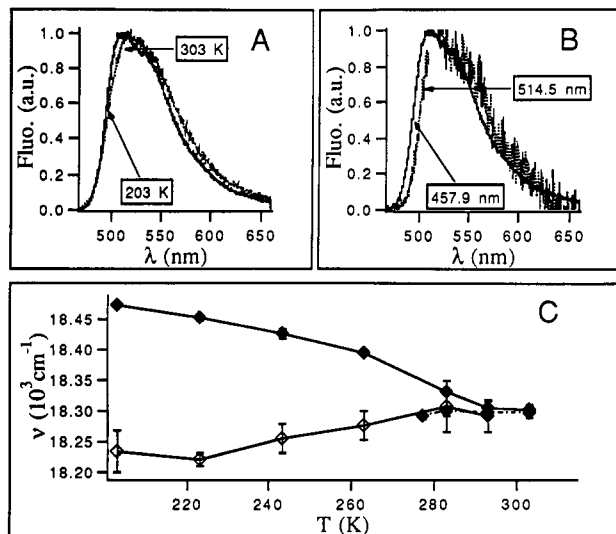


FIGURE 4: Temperature and excitation-wavelength dependence of emission spectra of the $\Delta 14$ deletion mutant of lipoamide dehydrogenase from *A. vinelandii*. (A) Temperature-dependent shift of emission spectra in 80% glycerol, 50 mM KP_i , pH 7.0, upon 457.9-nm excitation. (B) Excitation-wavelength-dependent shift of emission spectra at 203 K. The points between 512 and 519 nm contain a considerable amount of 514.5-nm laser scattering and were therefore omitted in the spectrum obtained after red-edge excitation. (C) Center of gravity of fluorescence spectrum expressed on a wavenumber scale as function of temperature and excitation wavelength: open symbols, 514.5-nm excitation; closed symbols, 457.9-nm excitation; solid lines, data obtained in 80% glycerol, 50 mM KP_i , pH 7.0; broken lines, data obtained in 50 mM KP_i , pH 7.0.

is converted from a solid-state environment (on a fluorescence time scale) at low temperature to a state with efficient dipolar relaxation ($\tau_r \ll \bar{\tau}_f$). Comparison of these results with the temperature and excitation-wavelength dependence of the wild type enzyme clearly shows that the deletion of the 14 C-terminal amino acids has a drastic effect on the dipolar re-

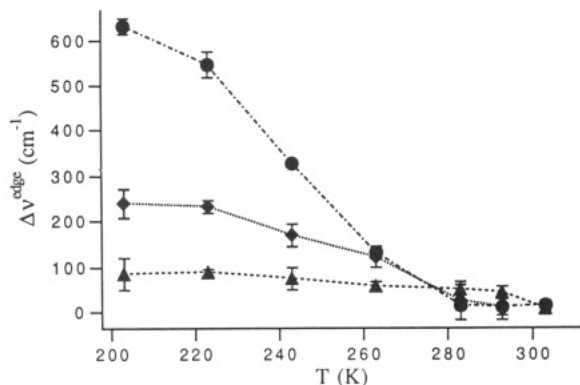


FIGURE 5: Difference between center of gravity of emission spectra obtained upon main-band and red-edge excitation as function of temperature in 80% glycerol: ●, FAD; ◆, LipDH-Δ14; ▲, LipDH-AV.

laxational properties of the active site.

Interpretation of the Data According to Continuous Relaxation Models. Upon red-edge excitation, a significant bathochromic shift of the emission spectra was observed in 80% glycerol at 203 K in the wild type enzyme whereas no clear shift could be detected in aqueous solution between 277 and 313 K. Furthermore, the spectra of the protein in aqueous solution were red-shifted relative to the spectra obtained in 80% glycerol at all measured temperatures. Since there is practically no interaction of the solvent dipoles with the isoalloxazines in this protein, the results indicate rapid dipolar relaxation in aqueous solution on the time scale of fluorescence emission ($\tau_r \ll \bar{\tau}_f$). Protein dynamics are considerably damped in 80% glycerol at 203 K, and dipolar relaxation is slowed down to a time scale beyond that of fluorescence emission. In this situation, the emission is observed from the nonequilibrium Franck-Condon excited states and the bathochromic shift upon edge excitation is related to the inhomogeneous bandwidth of the spectra reflecting the structural disorder of the dipoles in the neighborhood of the isoalloxazines. From the plot of $\Delta\nu^{\text{edge}}$ as a function of temperature (Figure 5) it can be seen that the edge shift at 203 K in LipDH-AV amounts to 100 cm^{-1} whereas 250 and 650 cm^{-1} were obtained for LipDH-Δ14 and free FAD, respectively. In the wild type enzymes the isoalloxazine thus exists in a highly ordered dipolar environment which exhibits small-amplitude fluctuations in a medium of low viscosity. In the absence of the 14 C-terminal amino acids of LipDH-AV, the solvent dipoles interact with isoalloxazine causing an increased disorder of the dipolar environment with a concomitant increase of the inhomogeneous bandwidth. From the ratio of $\Delta\nu^{\text{edge}}$ to its limiting value at low temperature (Figure 5), the dipolar relaxation time can be estimated by eq 2 when the average fluorescence lifetime ($\bar{\tau}_f$) as a function of temperature is known. The average fluorescence lifetimes are obtained from analysis of the fluorescence decays and are presented in Figure 6. The results and details of the analysis are presented elsewhere (Bastiaens et al., 1992). In 80% glycerol, both for free FAD and for that bound to LipDH-Δ14, fast dipolar relaxation ($\tau_r \ll \bar{\tau}_f$) is found at temperatures above 263 K whereas rapid relaxation is only found at 303 K for the wild type enzyme (Figure 7A). As mentioned in the preceding section, dipolar relaxation is fast ($\tau_r \ll \bar{\tau}_f$) in aqueous solution for both proteins. In this particular case, the center of gravity of the emission spectra must then coincide with the relaxed energy state (ν_∞ of the Bakshiev-Mazurenko model). The dipolar relaxation time of the proteins in 80% glycerol can then be estimated from the time-integrated continuous relaxation model of Bakshiev and Mazurenko (eq 1). Results of this procedure are

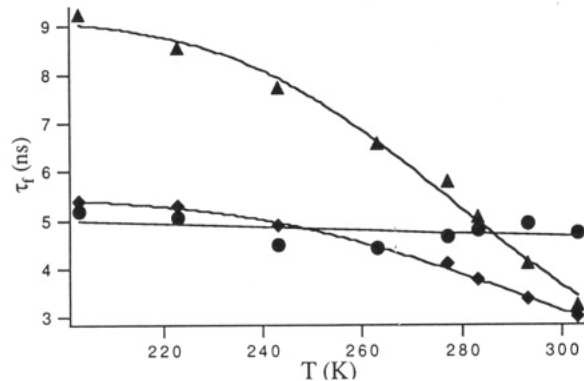


FIGURE 6: Average fluorescence lifetimes as function of temperature: ▲, LipDH-AV; ◆, LipDH-Δ14; ●, FAD; solid lines, best fit of data to eq 7.

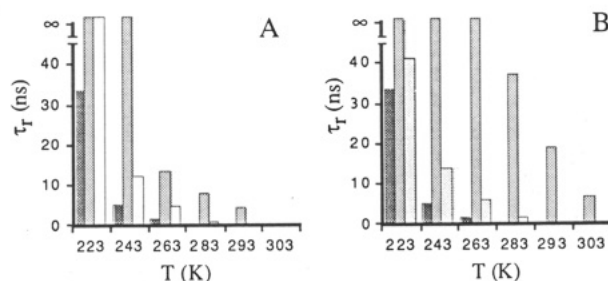


FIGURE 7: Dipolar relaxation times of free and protein-bound FAD in 80% glycerol. (A) Dipolar relaxation times as obtained from the modified Bakshiev-Mazurenko relation applying red-edge excitation (eq 2). (B) Dipolar relaxation times as obtained from the Bakshiev-Mazurenko relation (eq 1). From dark- to light-shaded columns or from left to right, FAD, LipDH-AV, and LipDH-Δ14. Each set of three columns refers to the temperature indicated on the abscissa.

displayed in Figure 7B. Comparison of the dipolar relaxation times, as obtained by the two methods (Figure 7A,B), shows that the results are comparable for FAD and LipDH-Δ14 but not for the wild type enzyme. In this enzyme the values of τ_r determined from eq 1 exceed those of the calculation based on eq 2. A possible cause for the discrepancy in the calculation of τ_r by the two methods is a temperature-dependent change of the selection function S (Nemkovich et al., 1991). This parameter is a measure of the photoselection of nonequilibrium solvates, defined as the ratio of the number of nonequilibrium to the number of equilibrium excited states, immediately after excitation. S will decrease with an increase of the homogeneous bandwidth ($\delta\nu$) relative to the inhomogeneous bandwidth ($\Delta\nu$). The increase of $\delta\nu$ is caused by the increase of the Boltzmann population of vibronic energy levels with temperature. With a decrease of S , the photoselection of nonequilibrium solvates will be less favored than that of equilibrium solvates, resulting in a smaller apparent magnitude of $\Delta\nu^{\text{edge}}$. This decrease will result in an underestimation of the dipolar relaxation time as calculated from eq 2. When $\Delta\nu \ll \delta\nu$ (as for the wild type enzyme), the error in the estimation of τ_r by eq 2 due to a change of S with temperature becomes considerable and τ_r cannot be determined. In this case, the Bakshiev-Mazurenko model (eq 1) will lead to a better estimation of τ_r provided that the value of the relaxed energy state is known.

The activation energies of dipolar relaxation as determined from τ_r calculated by eq 1 on Arrhenius coordinates (Figure 8) was 62 ± 10 kJ/mol for LipDH-AV (three points) and 47 ± 3 kJ/mol for free FAD in 80% glycerol. In an Arrhenius plot of the dipolar relaxation times of LipDH-Δ14, a breakpoint is observed which is not present for free FAD (Figure 8). This nonlinearity can be interpreted as originating from

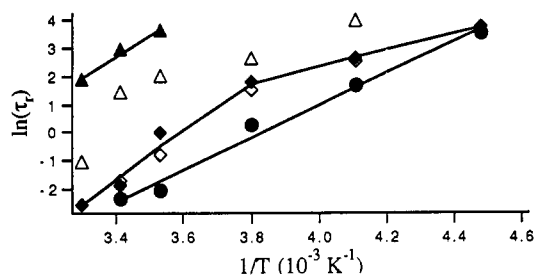


FIGURE 8: Dipolar relaxation times on Arrhenius coordinates: open symbols, τ_r as obtained from eq 2; closed symbols, τ_r as obtained from eq 1; \blacktriangle , LipDH-AV; \blacklozenge , LipDH-Δ14, \bullet , free FAD in 80% glycerol, 50 mM KP_i , pH 7.0; solid lines, linear fit of the data.

Table II: Thermal Quenching of Average Fluorescence Lifetime of Free and Bound FAD

	k_f^0 (MHz)	k_f^1 (THz)	E_f (kJ/mol)
LipDH-AV	109 ± 3	2.7 ± 2.6	24.2 ± 2.4
LipDH-Δ14	183 ± 2	0.55 ± 0.33	20.7 ± 1.5
FAD	189 ± 25		

a temperature-induced conformational change, but a more probable interpretation is that the isoalloxazines interact with two types of (dipolar) environments with different relaxational properties. To each of the environments (*i*), one can attribute a characteristic dipolar relaxation time τ_r^i whose dependence on temperature (*T*) is governed by an Arrhenius relation:

$$1/\tau_r^i = k_r^i \exp(-E_r^i/RT) \quad (6)$$

where k_r^i is the frequency factor (ns^{-1}), E_r^i the activation energy of relaxation of environment *i* (kJ/mol), and *R* the gas constant ($8.31 \text{ J mol}^{-1} \text{ K}^{-1}$). The thermal quenching of the fluorescence can be described by a temperature-dependent and a temperature-independent rate process (Bushueva et al., 1977):

$$1/\bar{\tau}_f = k_f^0 + k_f^1 \exp(-E_f/RT) \quad (7)$$

where $\bar{\tau}_f$ is the average fluorescence lifetime of the chromophore, k_f^0 the temperature-independent rate constant (ns^{-1}), k_f^1 the frequency factor (ns^{-1}), and E_f the activation energy of thermal quenching (kJ/mol).

Let us assume that the relative energy loss of the excited state ($\Delta\nu/\Delta\nu_0$ in the Bakshiev–Mazurenko relation) originates from several (*N*) independent relaxation processes of equal weight:

$$\Delta\nu/\Delta\nu_0 = \sum_{i=1}^N \frac{1}{N} \left(\tau_r^i / (\tau_r^i + \bar{\tau}_f) \right) \quad (8)$$

By substitution of relations 6 and 7 into eq 8 one obtains

$$\frac{\Delta\nu}{\Delta\nu_0} = \sum_{i=1}^N \frac{1}{N} \left[1 + \frac{k_r^i \exp[-E_r^i/RT]}{k_f^0 + k_f^1 \exp[-E_f/RT]} \right]^{-1} \quad (9)$$

The parameters k_f^0 , k_f^1 , and E_f are obtained from a time-resolved fluorescence experiment where the average fluorescence lifetime as a function of temperature is fitted to eq 7 (Figure 6). These parameters are collected in Table II. The average fluorescence lifetime of free FAD in 80% glycerol is temperature invariant in the measured temperature domain (Figure 6). In that case, only a temperature-independent rate constant is used to describe the thermal behavior of the fluorescence decay (Table II). The fluorescence decay parameters can be fixed in the subsequent analysis of the temperature-dependent energy loss of the excited state to a model describing a single ($N = 1$) relaxation process (two

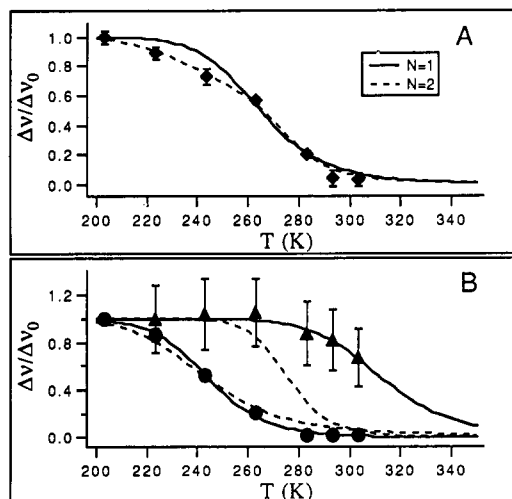


FIGURE 9: Relative energy loss ($\Delta\nu/\Delta\nu_0$) as function of temperature fitted to eq 9: (A) \blacklozenge , LipDH-Δ14 in 80% glycerol, 50 mM KP_i , pH 7.0; solid line, fit to a model with a single activation energy; broken line, fit to a model with two activation energies. (B) free FAD (\bullet) and LipDH-AV (\blacktriangle) in 80% glycerol, 50 mM KP_i , pH 7.0; solid line, fit to a model with single activation energy; broken lines, calculated energy losses of the individual relaxational processes in LipDH-Δ14 as obtained from the parameters of the best fit to a $N = 2$ model.

parameters: k_r^1 , E_r^1) or a double ($N = 2$) relaxation process (four parameters: k_r^1 , E_r^1 , k_r^2 , E_r^2). As can be seen in Figure 9A, we obtained an improved fit by assuming that relaxation in LipDH-Δ14 originates from two types of environments ($N = 2$, $\chi^2 = 1.56$) instead of one ($N = 1$, $\chi^2 = 15.6$). The recovered activation energies were 33 ± 14 (first environment) and 83 ± 7 kJ/mol (second environment). We performed a similar fit to the relative energy loss of free FAD in 80% glycerol assuming a single environment ($N = 1$, $\chi^2 = 4.9$) and obtained an activation energy of 43 ± 3 kJ/mol. This value is in close agreement with the value obtained from the slope of the Arrhenius plot (47 ± 3 kJ/mol, Figure 8), which shows the validity of the method. The temperature dependence of the individual relative energy losses ($\Delta\nu/\Delta\nu_0$) due to the relaxation of the two distinct environments in LipDH-Δ14 is plotted in Figure 9B together with data of the free chromophore and of the wild type enzyme in 80% glycerol. The similarity in shape of the curve and activation energy of the first environment with that of the free chromophore makes it tempting to assign the first type of relaxation in LipDH-Δ14 to solvent dipoles and the second to protein dipoles. For LipDH-AV we found an activation energy of 73 kJ/mol assuming a single environment ($N = 1$, $\chi^2 = 0.08$). However, the error in the activation energy was completely undetermined due to the small energy loss in the measured temperature region (Figure 9B). From these results we conclude that the activation energy of relaxation is relatively large (>70 kJ/mol), which indicates a rigid dipolar environment on a time scale of fluorescence of LipDH-AV in 80% glycerol.

DISCUSSION

With the steady-state iodide quenching experiments in aqueous solution, we demonstrated that the isoalloxazines in the wild type and deletion mutant of LipDH-AV are located in different environments. The larger bimolecular rate constant of quenching (k_q) in LipDH-Δ14 points to an enhanced solvent-accessible active site over the wild type enzyme. Although one may argue that a net negative charge in the vicinity of the isoalloxazines is the predominant factor which causes shielding of iodide ions in the wild type enzyme,

this is contradicted by the temperature invariance of the emission spectra in 80% glycerol in contrast to LipDH- Δ 14. If indeed the active site would be solvent accessible, one would expect the solvent dipoles to interact with the flavins causing temperature-dependent relaxational shifts as observed in LipDH- Δ 14. Another possible cause which could lead to an apparent increase of k_q in the deletion mutant is a larger dissociation constant of the FAD-apoenzyme complex. In that case a substantial fraction would be free in solution and accessible to iodide ions. This possibility can also be disregarded as (i) molecular sieve chromatography was applied prior to any measurement, (ii) the spectral parameters of the emission spectra of free FAD and that bound to LipDH- Δ 14 are different, (iii) the Stern-Volmer plot of the Δ 14 mutant does not exhibit concave upward behavior, which is typical for two classes of fluorophores with different accessibility, (Lehrer, 1971), and (iv) energy transfer between the cofactors in the mutant protein is observed, indicating that FAD is still bound and the $\alpha\alpha$ -quaternary structure preserved (Bastiaens et al., 1992).

The local electronic relaxational properties of the flavins in the deletion mutant were shown to be different from the wild type enzyme although the gross structure is conserved (Schulze et al., 1991). By red-edge excitation at 203 K, we found a small inhomogeneous bandwidth in the wild type enzyme (≈ 100 – 150 cm^{-1}) which was substantially larger in LipDH- Δ 14 (≈ 250 cm^{-1}) (Figure 5). This observation reveals the highly structured character of the protein matrix in the vicinity of the flavins in the wild type enzyme. Exposure of the flavins to the isotropic dipole distribution of the solvent (as in the deletion mutant) creates an increase of the inhomogeneous bandwidth and a concomitant increase of the selection function upon red-edge excitation. Rapid dipolar relaxation between 203 and 303 K was only found in LipDH- Δ 14, where we could resolve two independent relaxational processes. One process with the lower activation energy (≈ 30 – 45 kJ/mol) was assigned to solvent relaxation and the other with the larger activation energy (≈ 80 kJ/mol) to protein dipole relaxation. If dipolar relaxation is coupled to the dynamic properties of the protein, the latter higher activation energy reflects the ordered rigid protein structure in the vicinity of the active site. In LipDH-AV, where the flavin is predominantly surrounded by protein dipoles, dipolar relaxation in 80% glycerol was ineffective ($\tau_r \gg \tau_f$) in the measured temperature interval. The activation energy of relaxation (> 70 kJ/mol) was of the same order as that found for one of the relaxational processes in LipDH- Δ 14, which is an indication that we are observing the same dynamic behavior of the protein matrix in both proteins in 80% glycerol. The removal of the 14 C-terminal amino acids has a most drastic effect on the Lip(SH₂) binding site, which comprises amino acid residues from both subunits (Mattevi et al., 1991; Schulze et al., 1991). Since the Lip(SH₂) binding site is composed of amino acid residues of both subunits and removal of the 14 C-terminal amino acids destabilizes the dimer, we expect that the C-terminal tail folds back into the Lip(SH₂) binding site thereby shielding the active site from the solvent. Both in the wild type enzyme and in the deletion mutant, rapid small-amplitude fluctuations of (protein) dipoles in the vicinity of the isoalloxazines take place in aqueous solution. It would then be of interest to investigate the coupling between enzyme catalysis and the dynamics of the active site by studying the effect of different viscogens on enzyme kinetic parameters and dipolar relaxation in these systems (Demchenko et al., 1989).

Another experimental method by which the dipolar relaxational properties of the active site can be investigated is by monitoring energy transfer between the flavin cofactors. From crystallographic data it is known that the isoalloxazine parts of the FADs are separated by approximately 3.9 nm (Mattevi et al., 1991). Calculation of the relevant parameters of the Förster equation shows that energy transfer between the cofactors is possible and measurable (Bastiaens et al., 1992). Both the excitation energy and the dipolar relaxational properties of the active sites will have a large influence on the efficiency of this process (Demchenko, 1987; Nemkovich et al., 1991). Upon main-band excitation, the efficiency of energy transfer in the wild type enzyme in 80% glycerol should be practically temperature invariant as the S_{0-1} transition energy of the flavins is approximately constant between 203 and 303 K (both absorption and emission spectra are indicative of that). In LipDH- Δ 14, however, energy transfer should become less efficient with an increase of temperature due to long-wavelength shift of the emission spectra, which causes a decrease in the overlap integral. The most drastic effects are expected upon red-edge excitation. Due to the small selection function in the wild type enzymes, the probability of energy transfer will hardly decrease upon edge excitation. Furthermore, the slow relaxational properties of the protein matrix will again cause a temperature invariance of this process. In contrast, the probability of energy transfer in LipDH- Δ 14 will drastically decrease upon edge excitation at low temperature (203 K) due to the substantial inhomogeneous broadening. Upon elevation of temperature, fast dipolar relaxation will cause both an increase and an excitation energy invariance in the efficiency of energy transfer. Such experiments corroborate the findings on the dynamic properties of the active sites as reported in this study (Bastiaens et al., 1992).

ACKNOWLEDGMENT

We thank Dr. C. Veeger for valuable discussions.

REFERENCES

- Bastiaens, P. I. H., van Hoek, A., Benen, J. A. E., Brochon, J. C., & Visser, A. J. W. G. (1992) *Biophys. J.* (in press).
- Bushueva, T. L., Busel, E. P., & Burstein, E. A. (1977) *Biochim. Biophys. Acta.* 534, 441–452.
- Demchenko, A. P. (1982) *Biophys. Chem.* 15, 101–109.
- Demchenko, A. P. (1985) *FEBS Lett.* 182, 99–102.
- Demchenko, A. P. (1986) *Essays Biochem.* 22, 120–157.
- Demchenko, A. P. (1987) *Ultraviolet Spectroscopy of Proteins*, pp 183–197, Springer-Verlag, Berlin.
- Demchenko, A. P. (1988a) *Trends Biochem. Sci.* 13, 374–377.
- Demchenko, A. P. (1988b) *Eur. Biophys. J.* 16, 121–129.
- Demchenko, A. P., Rusyn, O. I., & Saburova, E. A. (1989) *Biochim. Biophys. Acta* 998, 196–203.
- Eftink, M. R. & Ghiron, C. A. (1981) *Anal. Biochem.* 114, 199–227.
- Galley, W. C., & Purkey, R. M. (1970) *Proc. Natl. Acad. Sci. U.S.A.* 67, 1116–1121.
- Lehrer, S. S. (1971) *Biochemistry* 10, 3254–3263.
- MacGregor, R. B., & Weber, G. (1981) *Ann. N.Y. Acad. Sci.* 366, 140–154.
- MacGregor, R. B., & Weber, G. (1986) *Nature* 319, 70–73.
- Mattevi, A., Schierbeek, A. J., & Hol, W. G. J. (1991) *J. Mol. Biol.* 220, 975–994.
- Mazurenko, Y. T.; Bakhshiev, N. G. (1970) *Opt. Spectrosc. (Engl. Transl.)* 28, 905–913.
- McCully, V., Burns, G., & Sokatch, J. R. (1986) *Biochem. J.* 233, 737–742.

- Nemkovich, N. A., Rubinov, A. N., & Tomin, V. I. (1991) Inhomogeneous Broadening of Electronic Spectra of Dye Molecules, in *Topics in Fluorescence Spectroscopy* (Lakowicz, J. R., Ed.) Vol. 2, pp 367–428, Plenum Press, New York.
- Reed, L. J., & Oliver, R. M. (1986) *Brookhaven Symp. Biol.* 21, 397–412.
- Rubinov, A. N.; Tomin, V. I. (1970) *Opt. Spectrosc. (Engl. Transl.)* 29, 1082–1086.
- Schierbeek, A. J., Swarte, M. B. A., Dijkstra, B. W., Vriend, G., Read, R. J., Hol, W. G. J., Drenth, J., & Betzel, C. (1989) *J. Mol. Biol.* 206, 365–379.
- Schulze, E., Benen, J. A. E., Westphal, A. H., de Kok, A. (1991) *Eur. J. Biochem.* 200, 29–34.
- Teale, F. W. J. (1960) *Biochem. J.* 76, 381–388.
- Visser, A. J. W. G. (1984) *Photochem. Photobiol.* 40, 703–706.
- Visser, A. J. W. G. (1989) Time-Resolved Fluorescence Studies of Flavins, in *Fluorescent Biomolecules* (Jameson, D. M., & Reinhart, D., Eds.) pp 319–341, Plenum Press, New York.
- Visser, A. J. W. G., & Müller, F. (1979) *Helv. Chim. Acta.* 62, 593–608.
- Visser, A. J. W. G., Grande, H. J., Müller, F. & Veeger, C. (1974) *Eur. J. Biochem.* 45, 99–107.
- Visser, A. J. W. G., Penners, N. H. G., van Berkel, W. J. H., & Müller, F. (1984) *Eur. J. Biochem.* 143, 189–197.
- Weber, G. (1950) *Biochem. J.* 47, 114–121.
- Weber, G. (1960) *Biochem. J.* 75, 335–345.
- Westphal, A. H., & de Kok, A. (1988) *Eur. J. Biochem.* 172, 299–305.
- Williams, C. H., Jr. (1976) *Enzymes (3rd Ed.)* 13, 89–173.
- Registry No.** FAD, 146-14-5; LipDH, 9001-18-7; FMN, 146-17-8; dihydrolipoamide, 462-20-4.